In-Tube Condensation of Zeotropic Refrigerant R454C from Superheated Vapor to Subcooled Liquid

Tabeel A. Jacob[a] and Brian M. Fronk[a]*

[a] *School of Mechanical, Industrial and Manufacturing Engineering*
Oregon State University
Corvallis, OR 97331, USA,

* Corresponding Author: Email: Brian.Fronk@oregonstate.edu

Tabeel A. Jacob (Student Member ASHRAE) is a graduate research assistant in the School of Mechanical, Manufacturing and Mechanical Engineering (MIME), Oregon State University, Corvallis, OR. Brian M. Fronk (Associate Member ASHRAE) is an assistant professor in the School of MIME, Oregon State University, Corvallis, OR

In-Tube Condensation of Zeotropic Refrigerant R454C from Superheated Vapor to Subcooled Liquid

ABSTRACT

This paper investigates the in-tube, superheated, saturated and subcooled condensation of zeotropic refrigerant mixture R454C. R454C is proposed to replace R404A for commercial refrigeration applications. Quasi-local heat transfer coefficients were measured in a 4.7 mm horizontal tube at mass fluxes ranging from 100 – 500 kg m^{-2} s^{-1} at three different saturation conditions (40, 50 and 50 °C). The resulting data was compared with the non-equilibrium condensation models of Agarwal & Hrnjak (2014), Kondou & Hrnjak (2012) and Xiao & Hrnjak (2017), as well as the equilibrium model of Cavallini et al. (2006) with the Gnielinski (1976) correlation for predictions in subcooled and saturated regions. The additional mass transfer effects were accounted for by applying the Silver (1947), Bell & Ghaly (1973) mixture correction. The non-equilibrium Kondou & Hrnjak (2012) model, with the predictions in the subcooled region from Gnielinski (1976) correlation, agrees best with the data (mean average percent error = 9%). An air-cooled condenser for a 1055 kW refrigeration system is designed by following both the non-equilibrium and equilibrium approaches. This non-equilibrium approach leads to a 4.8% and 9.1% reduction in heat transfer area for R454C and R404A, respectively. R454C condenser area is 17-21% larger than that of a R404A condenser.

INTRODUCTION

Flammability, decreased system performance and increased equipment size are some of the critical risks of implementing new, lower global warming potential (GWP) refrigerants in the heating, ventilation, air conditioning, and refrigeration (HVAC&R) industry. To mitigate the flammability risk, refrigerant manufacturers have introduced a suite of new working fluids consisting of zeotropic mixtures of hydrofluorocarbons (HFC), hydrofluoroolefins (HFO), and other fluids. On one hand, the tailored mixtures can achieve lower global warming potential than HFCs such as R404A, while also reducing the flammability compared to low GWP pure fluids such as R32. On the other hand, the zeotropic mixtures behavior of these fluids complicates the phase change heat transfer behavior and can lead to degraded heat transfer and larger heat exchangers. Deploying these new refrigerant mixtures requires detailed understanding of the phase change behavior and validation of the applicability of models and correlations for predicting heat transfer.

Conventionally, the heat transfer in a condenser is modeled by assuming a local thermodynamic equilibrium and then categorizing the flow as either superheated vapor, saturated two-phase flow, or subcooled liquid based on the specific bulk enthalpy. Single- or two-phase heat transfer correlations are then used depending on the expected flow regime. However, past experiments on the cooling of pure superheated refrigerants have shown that this assumption does not accurately describe the actual heat transfer mechanisms (Agarwal & Hrnjak, 2014; Kondou & Hrnjak, 2012). Vapor begins to condense as soon as the wall temperature drops below the saturation temperature, even when the bulk enthalpy is above the saturation vapor enthalpy. In this so-called superheated condensation region, the measured local heat transfer coefficients are much greater than those predicted by single-phase correlations. The superheated condensation region is

of increasing importance due to the growing interest in high-temperature heat pumps and heat pump water heaters, where the refrigerant superheating from the compressor outlet may be as high as 35°C (Arpagaus et al., 2018) and the desuperheating load is significant.

Furthermore, some of the refrigerants being proposed for application in high temperature heat pumps are zeotropic refrigerants mixtures (Zhang et al., 2010). During constant pressure condensation, these mixtures they exhibit a temperature glide (ΔT_{glide}) between the dew point and bubble point, due to the differences in saturation temperatures of the individual components (Fronk & Garimella, 2013). Preferential condensation of the less volatile components and the accumulation of the more volatile component at the liquid-vapor interface occurs, resulting in development of vapor and liquid concentration gradients. An additional mass transfer resistance to the process and a depression of the local liquid-vapor interface temperature is observed (which results in a lower driving temperature difference for the process). Consequently, condensation correlations for pure fluids cannot be accurately used to predict mixture condensation. Recent studies on the condensation of HFO mixtures have reported a lower heat transfer performance for mixtures compared to their individual components (Azzolin et al., 2019; Jacob et al., 2019).

Previous researchers have introduced frameworks to predict the heat transfer of multi-component refrigerants in the saturated two-phase region (Bell & Ghaly, 1973; Silver, 1947). However, there is a lack of publicly available experimental condensation data for the newer HFC/HFO refrigerant mixtures which can be used to validate these existing mixture condensation models. Similarly, past investigators (Agarwal & Hrnjak, 2014; Kondou & Hrnjak, 2012; Xiao & Hrnjak, 2017) have proposed non-equilibrium models to predict the condensation of pure fluids, including superheated, saturated and subcooled condensation. However, the condensation of refrigerant mixtures in the superheated and subcooled regions remains relatively unaddressed in

the literature. The mixture effects for zeotropic refrigerants are most pronounced at relatively high qualities, which is also when the effects of superheated condensation are observed. Therefore, it is critical to investigate the condensation of refrigerant mixtures during the complete condensation process through the superheated, saturated and subcooled regions, and understand the applicability of models that account for non-equilibrium condensation phenomena.

This study is focused on the HFO/HFC zeotropic mixture R454C, proposed as a replacement for R404A in medium temperature commercial and industrial refrigeration systems. R454C is a binary mixture of R32 (HFC) and R1234yf (HFO) with a mass composition equal to 21.5% and 78.5%, respectively. It has a temperature glide of approximately 6.5 K at typical condenser conditions and has been classified as an A2L mildly flammable refrigerant mixture by ASHRAE (ASHRAE, 2017). Mitigating the flammability risks associated with HFO refrigerants is an important design consideration which requires further exploration in parallel with the heat transfer investigations (Wu et al., 2019). Table 1 shows a comparison of the thermodynamics properties of the R404A and R454C at a dew point temperature equal to 50 °C, from REFPROP 10 (Lemmon et al., 2018). Due to its higher latent heat of vaporization, higher liquid thermal conductivity and approximately 96% lower GWP, R454C shows promise as a replacement candidate for R404A. However, before deployment as an R404A replacement, it is critical to investigate its condensation heat transfer to determine the role of mixture effects through the superheated, saturated and subcooled condensation regions, as discussed above.

Therefore, in the current study, we experimentally measure the quasi-local heat transfer coefficients for condensing R454C from a superheated vapor to a subcooled liquid. We compare the measured data with available single-phase and condensation correlations from the literature, with and without corrections accounting for mixture effects. Based on the resulting agreement,

recommendations for predicting complete condensation for refrigerant mixture R454C are provided. Finally, the performance of R404A and R454C is compared by designing a representative air-cooled condenser for a 1055 kW refrigeration system and determining the total heat transfer area required for each refrigerant.

Table 1 Thermodynamic Properties Of R404A And R454C At T_{dew} = 50 °C, From REFPROP 10 (Lemmon et al., 2018)

	R404A	R454C
ASHRAE Classification (ASHRAE, 2017)	A1	A2L
GWP (ASHRAE, 2017)	3943	148
Temperature glide (°C)	0.3	6.5
Saturation pressure (kPa)	2296	1870
Latent heat of vaporization (kJ kg^{-1})	103	133
Liquid density (kg m^{-3})	899	924
Vapor density (kg m^{-3})	138	91
Liquid viscosity × 10^6 (kg m^{-2} s^{-1})	86.5	92.8
Vapor viscosity × 10^6 (kg m^{-2} s^{-1})	14.5	13.8
Liquid conductivity × 10^3 (W m^{-1} K^{-1})	52.7	65.7
Surface tension × 10^3 (N m^{-1})	1.7	2.6

PRIOR WORK

Mota-Babiloni et al. (2018) investigated the feasibility of replacing R404A with the low GWP refrigerants R454C and R455A in a fully instrumented vapor compression refrigeration system. Tests were performed to simulate operating conditions in warmer climates, at condensing temperatures equal to 32, 39.5, 47.5 °C and evaporating temperatures of -30, -21.5, -13 °C. They found the cooling capacity of R454C to be comparable with R404A, and the COP of R454C to be 15% higher. Therefore, from a system perspective, R454C was deemed an appropriate low GWP substitute for the R404A.

While the research of Mota-Babiloni et al. (2018) shows positive results at a full system level, at present there are no published studies available on condensation phenomena of R454C,

necessary for the design and optimization of next generation equipment. While there is limited data on R454C, the in-tube condensation of HFC/HFO refrigerant mixtures has received much recent attention in the quest to find the best low GWP fluids. We review these studies below, followed by a presentation of non-equilibrium condensation of refrigerants in general.

Condensation of Low GWP Zeotropic Mixtures

Azzolin et al. (2019) investigated the condensation heat transfer coefficients and two-phase frictional pressure drop of R455A (R32, R1234yf and R744 at 21.5/75.5/3.0% by mass) and R452B (R32, R1234yf and R125 at 67.0/26.0/7.0% by mass) inside a 0.96 mm and an 8 mm tube. The temperature glide for R455A and R452B are 9.8 °C and 1.1 °C, respectively. Azzolin et al. (2019) found the heat transfer coefficient of R452B to be higher than that of R455A, which was due to an increased contribution of mixture effects and a higher liquid conductivity. In general, the degradation due to mixture effects becomes increasingly pronounced with an increase in the temperature glide (Fronk & Garimella, 2013). The heat transfer coefficients for both refrigerants and diameters were predicted well by the (Cavallini et al., 2006) with the Silver (1947), Bell & Ghaly (1973) methodology (also known as the SBG method) used to correct for the additional heat and mass transfer resistances.

The SBG method can be used to account for the mixture effects associated with zeotropic condensation. With this method, the additional resistance due to mass transfer is correlated to a sensible vapor phase resistance. The resulting expression for mixture heat transfer coefficient is:

$$\alpha_{mix} = \left[\frac{1}{\alpha_{cond}} + \frac{\dot{Q}_{s,v}}{\dot{Q}_T} \frac{1}{\alpha_v} \right]^{-1} \tag{1}$$

Here, the α_{cond} is evaluated using two-phase correlations, while the sensible vapor heat transfer coefficient α_v is evaluated using the Dittus & Boelter (1930) correlation. The ratio of sensible heat load over the total heat load ($\dot{Q}_{s,v}/\dot{Q}_T$) is estimated as:

$$\frac{\dot{Q}_{s,v}}{\dot{Q}_T} \approx \frac{x c_{p,v} \Delta T_{glide}}{h_{lv}} \tag{2}$$

where x, $c_{p,v}$ and h_{fv} are the thermodynamic quality, vapor specific heat capacity and the latent heat of vaporization. The SBG method was originally developed for saturated condensation with equilibrium assumptions and has been widely used in the HVAC&R industry to predict refrigerant mixture condensation heat transfer (Cavallini et al., 2002; Davide Del Col et al., 2015; Kondou et al., 2015).

In our prior work (Jacob et al., 2020), we investigated the condensation of two different non-flammable (ASHRAE A1 classification) replacement candidates for R404A, and compared their performance to that of R404A. Refrigerant mixtures R448A and R452A have a GWP equal to 1360 and 1950, respectively. They are both zeotropic refrigerant mixtures with temperature glides equal to 4.2 °C and 2.9 °C. Experiments were conducted inside a 4.7 mm horizontal tube at mass fluxes ranging from 100 to 800 kg m^{-2} s^{-1}, and at three different saturation conditions (40, 50, and 60 °C). The measured experimental saturated data for all three refrigerants was best predicted by the Cavallini et al. (2006) correlation, after accounting for the mixture effects using the SBG correction. Additionally, the heat transfer performance of all three refrigerants was compared for both equal mass fluxes and equal cooling capacities. The results indicate that both R448A and R452A may be considered appropriate substitutes for R404A from a heat transfer and two-phase frictional pressure perspective. However, compared to R448A and R452A, R454C offers a significant advantage in terms of a lower GWP.

Non-equilibrium condensation of pure fluids

One of the earliest theoretical models on superheated condensation was presented by Webb (1998). In his paper, Webb mentions the surprising lack of prior literature available on superheated condensation. He proposed that the heat transferred to a condensing superheated vapor, flowing inside of a tube, could be modeled as the sum of the sensible and latent component.

$$q''_{superheat} = q''_{sensible} + q''_{latent} \tag{3}$$

Equation 4 can be further rewritten in terms of the sensible and latent heat transfer coefficients, and their respective driving temperature differences:

$$\alpha_{superheat}\left(T_{sat} - T_{wall}\right) = \alpha_{sensible}\left(T_b - T_{sat}\right) + \alpha_{latent}\left(T_{sat} - T_{wall}\right) \tag{4}$$

where T_b and T_{wall} are the refrigerant bulk and tube wall temperatures. The sensible and latent heat transfer coefficients may be predicted using the Dittus & Boelter (1930) and Shah (1979) correlations, respectively. The framework proposed by Webb (1998) was a preliminary effort on the topic and was not rigorously validated against experimental data. Furthermore, a procedure on how to predict the quality during superheated condensation was not included in the work. This quality is required as an input for two-phase condensation models.

Kondou & Hrnjak (2012) investigated heat transfer during cooling of pure superheated CO_2 and R410A in a 6.1 mm tube. The experiments were carried out for superheats ranging from 0 to 40 °C for reduced pressures from 0.55 to 0.95. Their results confirmed the existence of latent effects in the superheated condensation region, as the measured heat transfer coefficients were significantly higher than those predicted by the single-phase Gnielinski (1976) correlation. Kondou & Hrnjak (2012) modeled the heat transfer in this region in a similar manner as Webb (1998), except the driving temperature associated with superheated condensation heat transfer coefficient was modified to $\left(T_b - T_{wall}\right)$:

$$\alpha_{superheat}\left(T_b - T_{wall}\right) = \alpha_{sensible}\left(T_b - T_{sat}\right) + \alpha_{latent}\left(T_{sat} - T_{wall}\right) \tag{5}$$

Here, a constant quality of 0.9999 is assumed in the superheated region to determine the latent heat transfer coefficient from the Cavallini et al. (2006) correlation. Agarwal & Hrnjak (2014) improved the model by introducing the areas associated with the vapor core and liquid condensate:

$$\alpha_{superheat} A_i (T_b - T_w) = \alpha_{TP} A_i (T_{sat} - T_w) + \alpha_v A_v (T_b - T_{sat}) \tag{6}$$

While Kondou & Hrnjak (2012) and Agarwal & Hrnjak (2014) models were able to predict the superheated condensation heat transfer with a good agreement for pure HFC and HFO refrigerants, a major short coming of these early models was that they assumed a constant quality of 0.9999 in the superheated region. The true quality in this region decreases along the length of the condenser as condensation actively occurs, and the liquid condensate layer continues to grow. In an attempt to more accurately determine the local flow structures, Xiao & Hrnjak (2017) introduced the superficial quality:

$$x_{sup} = \frac{h - h_{end}}{h_{onset} - h_{end}} \tag{7}$$

where h_{onset} and h_{end} represent the bulk enthalpies at actual locations where condensation begins and ends (instead of the saturated vapor and liquid enthalpies), respectively. Xiao & Hrnjak (2017) developed the criteria for predicting both h_{onset} and h_{end}. The bulk onset temperature is evaluated by determining the location where the tube wall temperature is equal to the saturation temperature:

$$T_{b,onset} = T_{sat} + \frac{q''}{\alpha_v} \tag{8}$$

where α_v and q'' are the single-phase vapor heat transfer coefficient and heat flux right before condensation begins. The temperature at which condensation ends was empirically determined to be:

$$T_{b,end} = T_{sat} - 0.33\frac{q''}{\alpha_l} \tag{9}$$

They further introduced a complete condensation model to evaluate the film heat transfer coefficient in the superheated, saturated and subcooled condensation regions. The model was validated against a database containing condensation data for refrigerants R134a, R32, R1234ze(E), R410A and R744 at mass fluxes ranging from 100 to 200 kg m^{-2} s^{-1}. In addition, Xiao and Hrnjak modified the flow regime map of El Hajal et al. (2003) to account for non-equilibrium effects during condensation of pure fluids (Xiao & Hrnjak, 2019).

A review of the literature reveals limited research on superheated condensation, primarily by Hrnjak and coworkers. There are even less investigations that address superheated condensation of refrigerant mixtures. In our prior work, we presented superheated condensation results for multi-component refrigerants (R448A and R452A) with lower temperatures glides (Jacob & Fronk, 2020b). In general, the mixture effects are more pronounced for higher temperature glide mixtures (Fronk & Garimella, 2016). Thus, in this study, we explore in detail the effects of superheated condensation for the binary mixture, R454C.

EXPERIMENTAL APPROACH

In this section, we provide details of the experimental facility, measurement technique and the data reduction methodology used to obtain R454C heat transfer coefficients. Readers are further referred to Jacob et al. (2019) for details of validation procedure for the experimental technique and facility used in this study, which was carried out by performing a series of single-phase heat transfer and pressure drop tests, as well as conducting condensation experiments for a well-established pure fluid (R134a).

Experimental facility

The test facility and the measurement technique used in this study to investigate the condensation for R454C is the same as the one used in our prior work (Jacob et al., 2019, 2020).

Figure 1 shows the schematic and a photograph of the condensation facility. State point 1 marks the inlet of the test section where the refrigerant enters as a superheated vapor. The test section is a 1.6 m long tube-in-tube heat exchanger with a copper inner tube (ID = 4.7 mm, OD = 6.4 mm) and a polyvinyl chloride (PVC) outer tube (ID = 15.8 mm, OD = 21.3 mm). The refrigerant flows in the inner tube and is cooled by water flowing in the annulus in the counter flow direction. The test section is further divided into seven instrumented 19 cm long segments. The outer copper surface temperature and the inlet and outlet water temperature of each segment are measured to obtain quasi-local heat transfer coefficients along the length of the heat exchanger.

The refrigerant leaves the test section as a subcooled liquid. It is then further cooled in the post cooler between state point 2 and 3. The refrigerant is then pumped through the loop using a magnetically coupled gear pump. There is no lubricating oil present in the experiment. The pressure in the system is controlled using a piston accumulator, connected to a nitrogen tank with a pressure regulator. Before entering the test section, the refrigerant is superheated using three cartridge heaters, each with a 2300 W heating capacity. The power supplied to the heaters is adjusted for different tests using a silicon controlled rectifier (SCR). A static mixer is used to provide a well-mixed fluid at the test section inlet, and a sight glass ensures that that no liquid droplets are entrained in the flow.

Data reduction

For each experiment, the system was allowed to reach steady state, which occurred when the fluctuations in the temperature, absolute pressure, differential pressure and mass flow rate readings were less than 0.1 °C, 10 kPa, 0.1 kPa and 0.1 g s^{-1}, respectively, for a period of four minutes. Data were then collected for four minutes at 1 Hz. The quasi-local heat transfer coefficient for a given segment in the test section is defined as:

$$\alpha = \frac{\dot{Q} / A_{si}}{(T_b - T_{wall,inner})} \tag{10}$$

where $\dot{Q}, A_{si}, T_b, T_{w,inner}$ are the total heat transferred, inner surface area, bulk refrigerant temperature, and inner surface temperature of the copper tube in the segment. The condensation heat duty in each segment was calculated from a water-side energy balance on the water side:

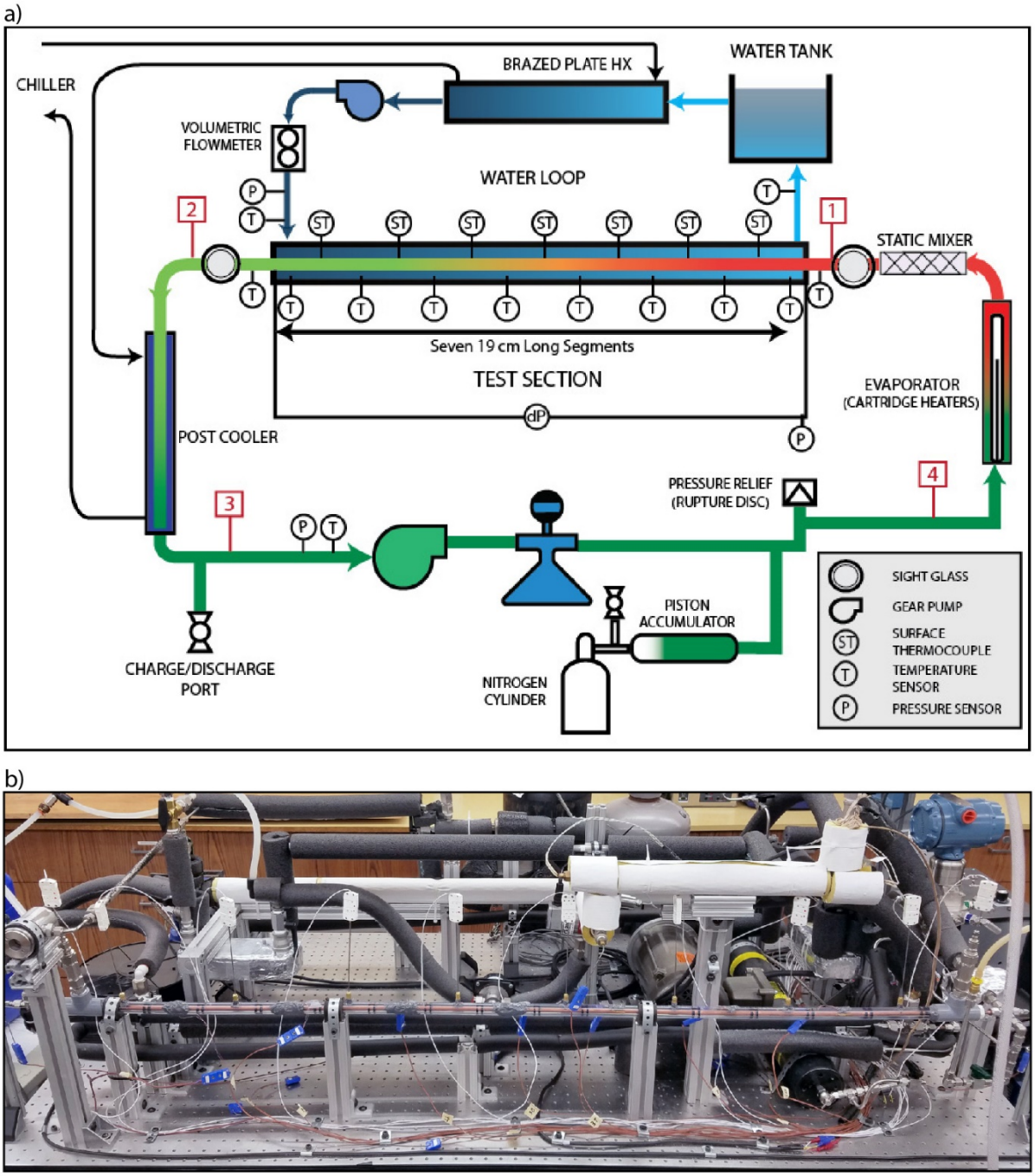

Figure 1 Condensation facility a) schematic b) photograph

$$\dot{Q} = \dot{m}_w (h_{w,in} - h_{w,out}) \tag{11}$$

where $\dot{m}_w$ is the water mass flow rate, and $h_{w,in}$ and $h_{w,out}$ are the inlet and outlet water enthalpies evaluated from the measured temperature and pressure. A detailed heat loss calculation from the

water-side accounting for thermal resistances in a segment due to convection through water, conduction through the PVC tubing (thickness = 0.55 cm) and polyethylene insulation (thickness = 1.9 cm), and air convection over the insulation showed that less than 0.2% difference in evaluated heat transfer coefficients, even after assigning a conservative ±200% uncertainty to the resistances. Additionally, the calculated heat lost by the refrigerant (evaluated using the measured test section inlet and outlet temperatures) was on average 1% (≈ 10 W) higher than the heat gained by water. Therefore, for simplicity, the heat gained by the water in a segment was assumed to be equal to the heat lost by the refrigerant. The refrigerant bulk specific enthalpy was tracked along the length of the tube using energy balances:

$$h_{r,out} = h_{r,in} - \frac{\dot{Q}}{\dot{m}_r} \tag{12}$$

The enthalpy of the superheated refrigerant at the test section inlet was evaluated based on the measured temperature and absolute pressure. The calculated segment refrigerant enthalpy, fixed refrigerant bulk concentration, and measured inlet absolute pressure were used to evaluate the refrigerant bulk equilibrium temperature and equilibrium thermodynamic quality (in the segments with two-phase flow) from REFPROP 10 (Lemmon et al., 2018):

$$T_{r,avg} = f(P, h_{r,avg}, y_1, y_2) \tag{13}$$

$$x_{r,avg} = f(P, h_{r,avg}, y_1, y_2) \tag{14}$$

The uncertainty due to the assumption of inlet pressure for evaluating local equilibrium was considered by evaluating the root mean square of the systematic uncertainty of the pressure sensor (Table 2) and the actual measured pressure drop for that data point. The root mean square value was then used as the new systematic uncertainty in the absolute pressure drop for all heat transfer calculations.

The inner tube wall temperature in Eq. 6 was determined using the measured outer wall surface temperatures and accounting for the thermal resistance through the tube wall. Axial conduction was neglected, since the thermal resistance in the axial direction was orders of magnitude higher than the resistance in the normal direction and thus, majority of the heat transfer occured in the normal direction. The heat transfer coefficient coefficients were then obtained from Eq. 6. Finally, the heat transfer data for R454C was collected at three different saturation conditions ($T_{sat,avg}$ = 40, 50 and 60 °C). The average saturation temperature ($T_{sat,avg}$) is defined as the average of bubble point and dew point temperatures.

Table 2 shows the list of systematic uncertainties and ranges of the sensors used in this study. The uncertainty propagation in the calculated variables from the measured variables is determined using the procedure suggested by Kline and McClintock (1953). The highest contribution to the uncertainty in heat transfer coefficients was from the water temperature measurements, which were measured using calibrated RTDs (±0.05 °C). The average and maximum uncertainties in the measured heat transfer coefficients were ±7% and ±13%, respectively.

Table 2 Ranges and uncertainties of the sensors

	Range	Uncertainty
RTD (water temperature)	-200 – 500 °C	±0.05 °C
Surface temperature	-200 – 500 °C	±0.5 °C
Type T thermocouple	-200 – 500 °C	±0.5 °C
Refrigerant mass flow meter	0 – 30 g s^{-1}	±0.1%
Water volumetric flow meter	0.04 – 7.5 L m^{-1}	±0.5%
Absolute pressure	0 – 10 MPa	±6 kPa
Differential pressure	0 – 62 kPa	±0.05 kPa

CONDENSATION RESULTS

We collected condensation data for R454C at three different saturation conditions ($T_{sat,avg}$ = 40, 50 and 60 °C) and at a range of mass fluxes (100 – 500 kg m^{-2} s^{-1}). For the experiments in

this study, the superheating at the test section inlet varied from 16 °C to 74 °C (Average = 45 °C). The resulting data were analyzed to obtain the quasi-local heat transfer coefficients associated with complete condensation from the superheated through saturated and subcooled regimes. The measured data is then compared against the predictions from various non-equilibrium and equilibrium condensation models. To facilitate the reproduction of this work and to guide future investigations on this topic, all measured and calculated variables from this study are publicly available in tabulated format in Jacob & Fronk (2020a).

Superheated Condensation

Figure 2 shows the plots of the temperature difference between dew point temperature and the inner tube wall surface temperature versus the bulk enthalpy in the so-called superheated region. For all the data points, the tube wall temperature is at least 20 °C lower than the dew point temperature. In addition, the heat transfer coefficients versus specific bulk enthalpy measured in the superheated condensation region at mass fluxes varying from 100 kg m^{-2} s^{-1} to 500 kg m^{-2} s^{-1} are also shown in Figure 2. The measured data points represent the heat transfer coefficients associated with segments upstream of the saturated two-phase region, which is why the associated bulk enthalpy is higher than the saturation enthalpy. As discussed earlier, the conventional approach would suggest that the heat transfer coefficients in this region can be modeled using single-phase heat transfer correlations. In this study, the inlet Reynolds number varied from 29,324 to 163,447, assuming pure vapor flow. Therefore, predictions from the Gnielinski (1976) correlation for single-phase turbulent heat transfer are also included in Figure 2 for the range of mass fluxes investigated. The measured heat transfer coefficients are significantly under-predicted by the single-phase Gnielinski (1976) correlation, suggesting the presence of “superheated” condensation. The heat transfer coefficients increase with increasing mass flux and decreasing

bulk enthalpy. For a given mass flux, they are maximum near the vapor saturation enthalpy. This is consistent with the results of Hrnjak and co-workers (Agarwal & Hrnjak, 2014; Kondou & Hrnjak, 2012; Xiao & Hrnjak, 2017). The results in Figure 2 and Table 3 further confirm the results of Hrnjak and co-workers (Agarwal & Hrnjak, 2014; Kondou & Hrnjak, 2012; Xiao & Hrnjak, 2017) that single-phase correlations are not an appropriate method to predict heat transfer coefficient in the superheated region. The superheated condensation models of Hrnjak and co-workers were developed for pure refrigerants. However, R454C is a zeotropic refrigerant mixture with a temperature glide of approximately 6.5 K for the range of saturation pressures in this study. One of the goals of the present study is to assess the application of these models to superheated mixture condensation and assess if the Silver, Bell and Ghaly (SBG) correction factor can be added to improve predictive capability. The measured data from Figure 2 were compared with the superheated condensation models, with and without considering the mixture effects using the SBG correction. Table 3 shows the comparison with three different superheated condensation models, as well as the single-phase Gnielinski (1976) correlation. The agreement is quantified in terms of the mean absolute percent error (MAPE) and the mean percent error (MPE).

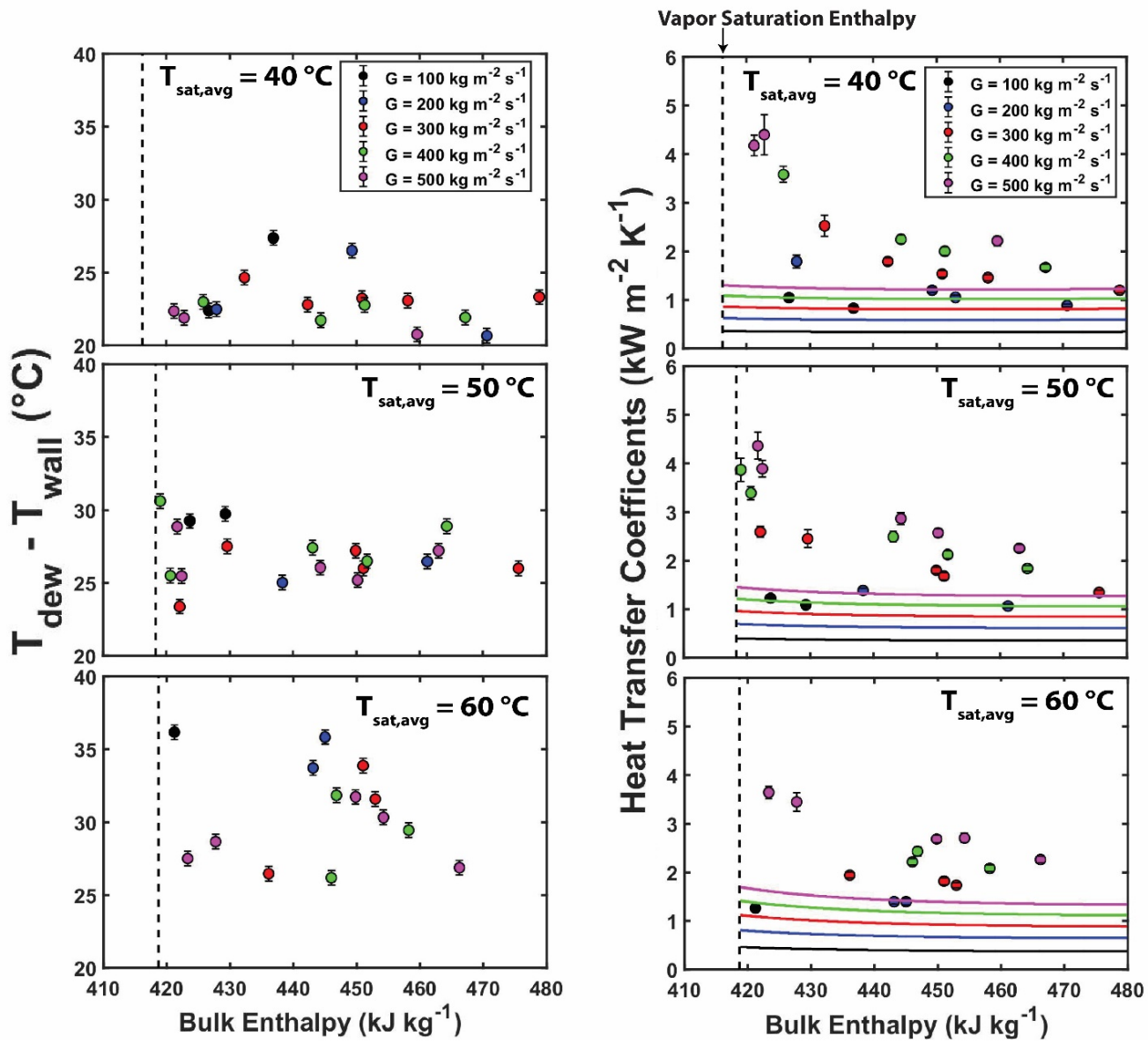

Figure 2 Left: temperature difference between dew point temperature and the inner tube wall surface temperature versus the bulk enthalpy. **Right:** Superheated condensation heat transfer coefficient versus bulk enthalpy for R454C at mass fluxes ranging from 100 to 500 kg m^{-2} s^{-1} and average saturation temperature of 40, 50 and 60 °C. The lines represent single-phase vapor heat transfer coefficients predicted using Gnielinski (1976) correlation.

Table 3: Predictive capability of different heat transfer models for R454C in the superheated region, with and without consideration of mixture effects

	Without SBG correction		**With SBG correction**	
	MAPE (%)	**MPE (%)**	**MAPE (%)**	**MPE (%)**
Gnielinski (1976)	53	-53	-	-
Kondou & Hrnjak (2012)	39	39	19	19
Agarwal & Hrnjak (2014)	36	36	17	17
Xiao & Hrnjak (2017a)	16	16	4	0

This comparison indicates that the model of Xiao & Hrnjak (2017a) is able to predict the superheated condensation data the best, with a MAPE equal to 16% without accounting for mixture effects. This model describes the local flow structure in the superheated region as annular and uses a modified form of Dittus & Boelter (1930) equation to determine the thermal resistance associated with the liquid film. This model has a similar structure as the Thome et al. (2003) model, which utilizes the film Reynolds number and corrects for the effects of interfacial roughness.

For all three models, the application of the SBG correction improved the predictive capabilities significantly. Specifically, the Xiao & Hrnjak (2017a) model with the SBG correction is able to predict the data the best, with a MAPE equal to 3.7%.

Saturated Condensation

Figure 3 shows the saturated condensation heat transfer coefficient versus the thermodynamic equilibrium quality for R454C at mass fluxes ranging from 100 to 500 kg m^{-2} s^{-1} and at an average saturation temperature equal to 40, 50 and 60 °C. The saturated condensation region exists in segments where the bulk enthalpy is higher than the liquid saturation enthalpy and lower than the vapor saturation enthalpy. These data were collected downstream of the location where the superheated condensation data was measured. The general trends in the data are consistent with the understanding of condensation from the literature. The heat transfer coefficient increases with the thermodynamic quality and mass flux, and decreases with the saturation temperature.

The measured data were compared with six different established correlations from the literature. Among these correlations are the Shah (2016) and Cavallini et al. (2006) correlation, which have been recommended in the ASHRAE Handbook: Fundamentals (ASHRAE, 2017) for predicting refrigerant condensation. The empirical Shah (2016) correlation is a revised version of

the highly cited Shah (1979) correlation. It was developed based on condensation data for 33 fluids in tubes with the internal diameters ranging from 0.1 to 49 mm, at a range of mass fluxes (1.1 to 1400 kg m^{-2} s^{-1}) and reduced pressures (0.0008 to 0.946). Based on his analysis, Shah (2016) identified three purely empirical regimes. Alternatively, the Cavallini et al. (2006) correlations categorizes the two-phase flows further into two different regimes: ΔT-Independent and ΔT-dependent. For ΔT-Independent flows, the heat transfer primarily occurs through a thin liquid condensate film on the inner tube surface. These regimes include shear dominated flows such as annular and intermittent flows. While for ΔT-Independent regimes, gravity is the dominant force, which causes a stratified liquid pool to develop at the bottom of the tube. For these regimes, the majority of heat transfer occurs at the top half of the tube. Similar to the Cavallini et al. (2006) correlations, the Thome et al. (2003) and Dobson & Chato (1998) correlations also model the condensation by categorizing the flows as either shear-dominated or gravity-dominated regimes. Garimella et al. (2016) investigated the heat transfer of nearly azeotropic refrigerant blends R404A and R410A at high reduced pressures (P_r = 0.8 -0.9) in tubes with the internal diameters ranging from 0.76 to 9.4 mm. At high reduced pressures, the ratio of liquid density over vapor density approaches unity and therefore, the contribution from interfacial shear to the total heat transfer becomes less significant. Garimella et al. (2016) introduced a new condensation heat transfer model to predict 91% of their data with less than ±25% error in the wavy, annular, and annular/wavy transition regimes. Del Col et al. (2005) extended the applicability of the Thome et al. (2003) correlation for refrigerant mixtures in the gravity dominated regimes by applying the SBG correction to both the film and liquid pool heat transfer coefficients.

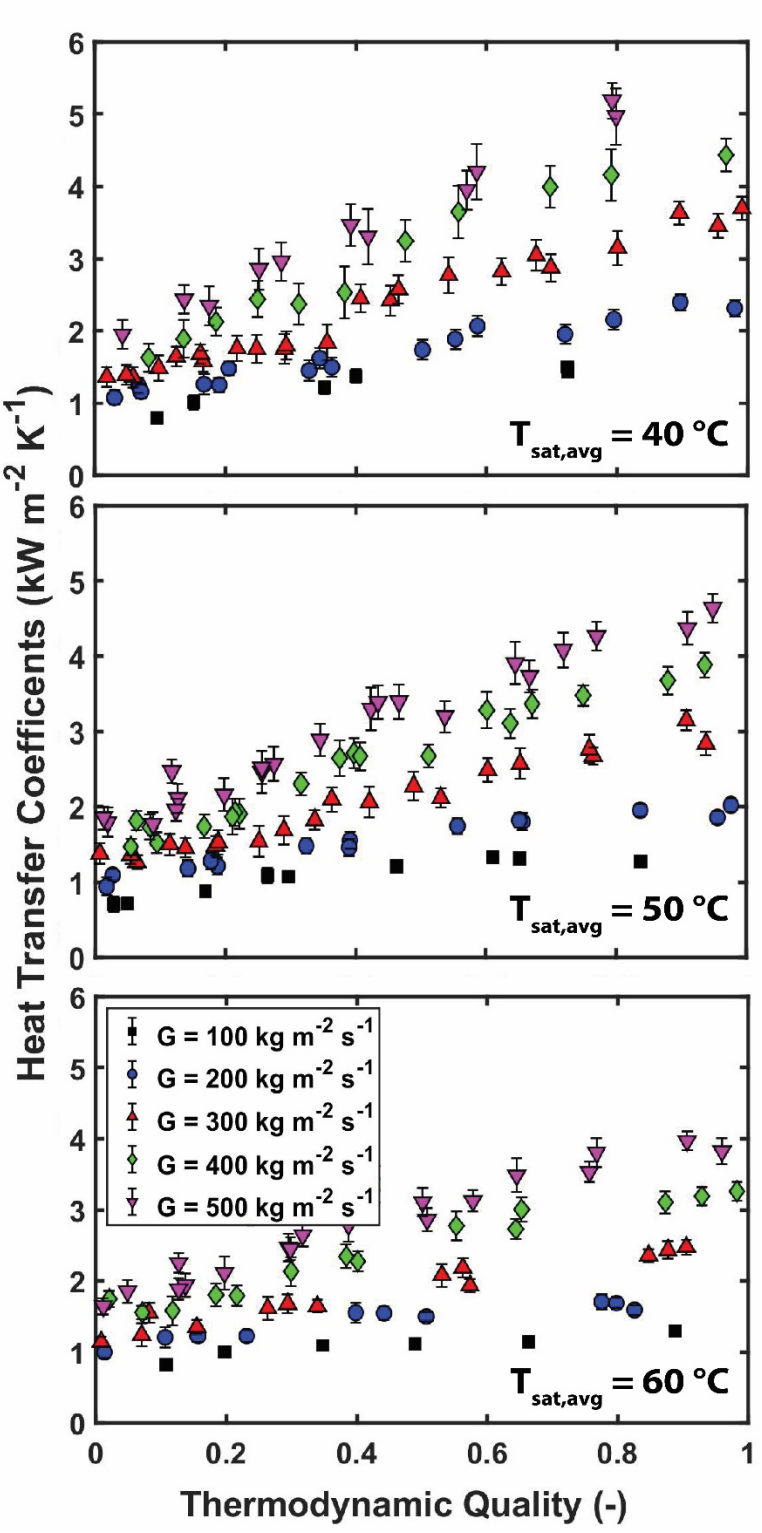

Figure 3 Saturated condensation heat transfer coefficient versus thermodynamic quality for R454C at G = 100 to 500 kg m^{-2} s^{-1} and at $T_{sat,avg}$ = 40, 50 and 60 °C.

The results are shown in Table 4. Among the correlations, the Cavallini et al. (2006) correlation predicts the data best, with the MAPE equal to 15% and 6% with and without SBG correction, respectively. The application of SBG correction on average lead to a 12% reduction in the predicted heat transfer coefficients from the Cavallini et al. (2006) correlation. For all the single component condensation correlations, the application of SBG correction improved the predictability. The Thome et al. (2003), Del Col et al. (2005), Garimella et al. (2016) and Shah (2016) correlations predict the data with reasonable accuracy, with MAPEs less than 15%. Overall, this analysis confirms that existing correlations with the SBG correction are accurately able to predict the saturated condensation of R454C.

Table 4: Predictive capability of different heat transfer models for R454C in the saturated region, with and without consideration of mixture effects

	Without SBG correction		**With SBG correction**	
	MAPE (%)	**MPE (%)**	**MAPE (%)**	**MPE (%)**
Shah (1979)	45	44	24	21
Dobson & Chato (1998)	33	29	16	9
Thome et al. (2003)	14	6	10	-3
Del Col et al. (2005)	-	-	10	-1
Cavallini et al. (2006)	15	13	6	-1
Shah (2016)	26	25	10	8
Garimella et al. (2016)	24	21	11	5

Subcooled Condensation

Figure 4 shows a comparison between the heat transfer coefficients measured in the subcooled region against those predicted by the single-phase Gnielinski (1976) correlations. The data agrees with the correlation extremely well, with the MAPE equal to 16%. Despite the good agreement with the single-phase correlation, this does not confirm or disprove the presence of latent effects in this region. A visualization study is required to conclude that. However, these results do indicate that the contribution of these latent effects to the heat transfer may be not significant. A comparison between the subcooled data and the complete condensation models is presented in the following section.

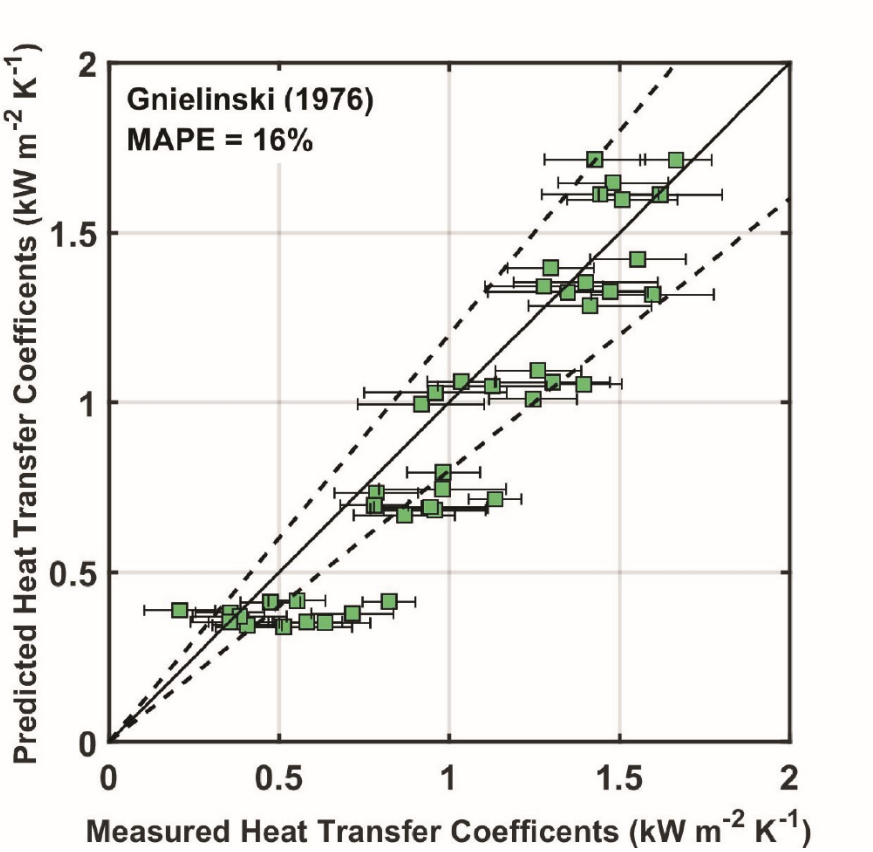

Figure 4 Measured heat transfer coefficients versus predictions from Gnielinski (1976) in the subcooled condensation regions.

Complete Condensation

To be generally applicable, a good heat transfer model must provide accurate predictions for not just the saturated condensation region, but also for the superheated and subcooled condensation regions. As shown earlier, the latent effects in these sections are significant. Therefore, we also compared the predictions from the models discussed above against our measured data for complete condensation.

Our experiments resulted in a total of a 312 data points. Among these data, 16% were superheated, 70% were saturated and 14% were subcooled condensation. These classifications were obtained using the criteria developed by Xiao & Hrnjak (2017a) for determining the onset and end of condensation. Among the two-phase models discussed in superheated condensation

section, the model of Kondou & Hrnjak (2012) does not provide predictions in the subcooled region. Therefore in order to compare each model with the complete data set, the Gnielinski (1976) correlation was used for predicting subcooled condensation with the Kondou & Hrnjak (2012) model. Similarly, it is insightful to compare the predictive capabilities of the traditional equilibrium approach (which ignores the latent effects in superheated and subcooled regions) against the non-equilibrium two-phase models. The Cavallini et al. (2006) correlation showed an excellent agreement with the saturated condensation data, with a MAPE equal to 6%. Therefore for the traditional approach, the saturated condensation data were predicted using the Cavallini et al. (2006) correlation, and the subcooled and superheated condensation data were predicted using the Gnielinski (1976) correlation. The results are shown in Figure 5 and summarized in Table 5.

The results show an opposite trend compared to that of the superheated condensation results. Overall, the Kondou & Hrnjak (2012) model with the Gnielinski (1976) correlation is able to predict the data the best, with a MAPE equal to 9%. This is partly due to the fact that Kondou & Hrnjak (2012) also recommended using the Cavallini et al. (2006) correlation for predictions in the saturated condensation region which, as noted earlier, predicts the saturated condensation data in this study very accurately. Conversely, the models of Agarwal & Hrnjak (2014) and Xiao & Hrnjak (2017a) significantly overpredict the data in the saturated region. This is consistent with Xiao's doctoral thesis (Xiao, 2019), where he reported that his non-equilibrium model significantly overpredicted the results for R32/R1234ze mixture condensation. He hypothesized that this is due to the steep temperature and concentration gradients in the liquid film which result in significant variations in the thermodynamic properties. These variations in the liquid film are not accounted for with the SBG correction.

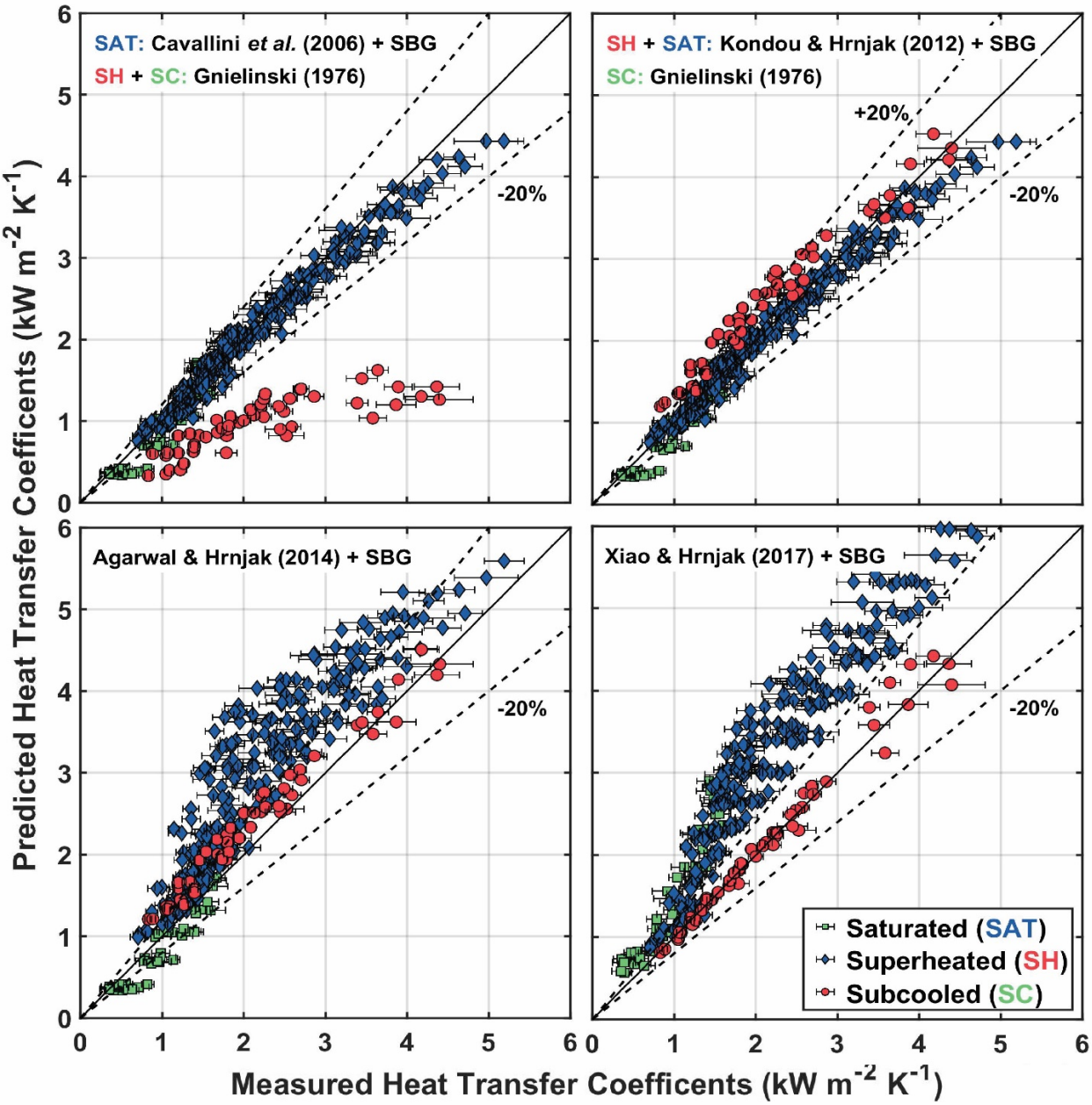

Figure 5 Measured heat transfer coefficients versus predictions from different models in the superheated, saturated and subcooled condensation regions.

Table 5: Predictive capability of different heat transfer models complete condensation including superheated, saturated and subcooled regions.

	With SBG correction	
	MAPE (%)	**MPE (%)**
Cavallini et al. (2006) + Gnielinski (1976)	15	-11
Kondou & Hrnjak (2012) + Gnielinski (1976)	9	1
Agarwal & Hrnjak (2014)	31	27
Xiao & Hrnjak (2017a)	40	40

It interesting to note that the overall MAPE for the traditional approach is lower than those associated with the models of Agarwal & Hrnjak (2014) and Xiao & Hrnjak (2017a), despite the poor agreement in the superheated region. This can be attributed to the poor performance in the saturated region of the Agarwal & Hrnjak (2014) and Xiao & Hrnjak (2017a) models. Furthermore, Figure 4 shows that using the single-phase heat transfer correlation to predict heat transfer in the subcooled region results in a relatively small error. However, there is a significant advantage of using the Kondou & Hrnjak (2012) with Gnielinski (1976) approach over the traditional approach due to the much better agreement in the superheated condensation region. This suggests that condensers with large desuperheating loads could be designed more accurately and compactly.

REFRIGERANT COMPARISON AND CONDENSER DESIGN

Since R454C has been proposed as a replacement for R404A, it is insightful to compare the performance of the two refrigerants with each other. R404A condensation data, measured as part of our prior work (Jacob et al., 2020), was used here for comparison. Figure 6 shows plots of saturated heat transfer coefficients for both the refrigerants at two different saturation temperatures (40 and 60 °C) and at a range of mass fluxes (200 to 500 kg m^{-2} s^{-1}). The results show that the heat transfer coefficients of both the refrigerants are similar in magnitude, with the heat transfer coefficients of R454C being slightly higher. This is primarily due to R454C's 24% higher liquid thermal conductivity (Table 1). However, the impact of degradation due to mixture effects for R454C is evident. The Cavallini et al. (2006) correlation is also able to predict the R404A data well, with the MAPE equal to 9%.

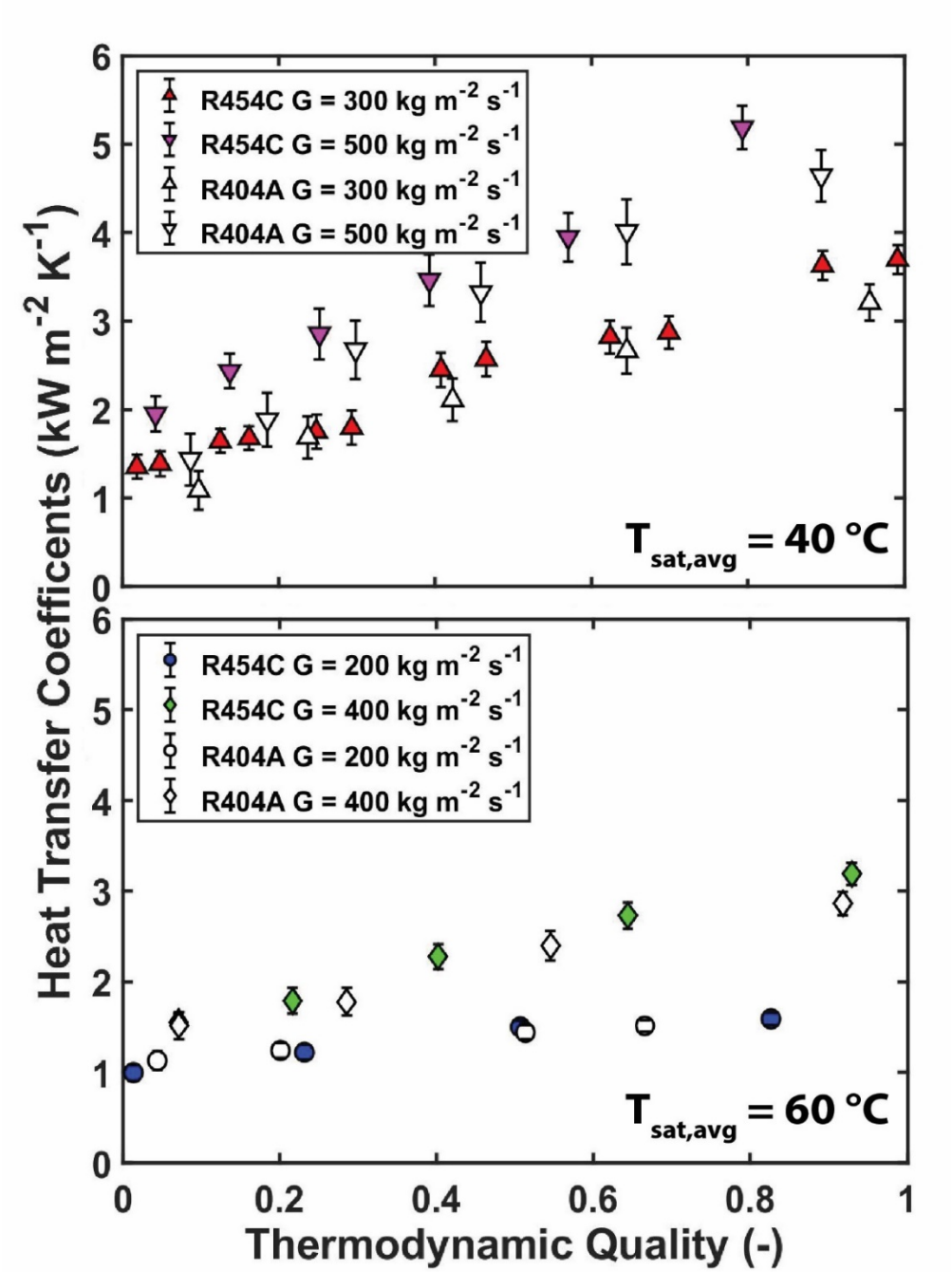

Figure 6 Condensation heat transfer coefficients versus thermodynamic quality of R454C and R404A at two different saturation temperatures (40 and 60 °C) and at a range of mass fluxes (200 to 500 kg m^{-2} s^{-1}).

Similarly, it is also insightful to compare the performance and sizes of these two refrigerants for an actual vapor compression system utilizing these fluids. We designed an A-frame air-cooled condenser (ACC) for a commercial refrigeration system with a 1055 kW (300 RT)

cooling capacity. The refrigerant evaporates and condenses at 0 °C and 40 °C, respectively, with the ambient temperature equal to 25 °C. A schematic of the ACC is shown in Figure 7. The ACC is cooled by air convection from an electrically driven fan. The size and geometry of the fins and tubes are informed by the investigation of Kays & London (1984), who collected experimental data for air-cooled heat exchangers. The air-side heat transfer coefficient was evaluated to be 52 W m^{-2} K^{-1} (Kays and London 1984), by assuming a constant air face velocity equal to 1 m s^{-1}.

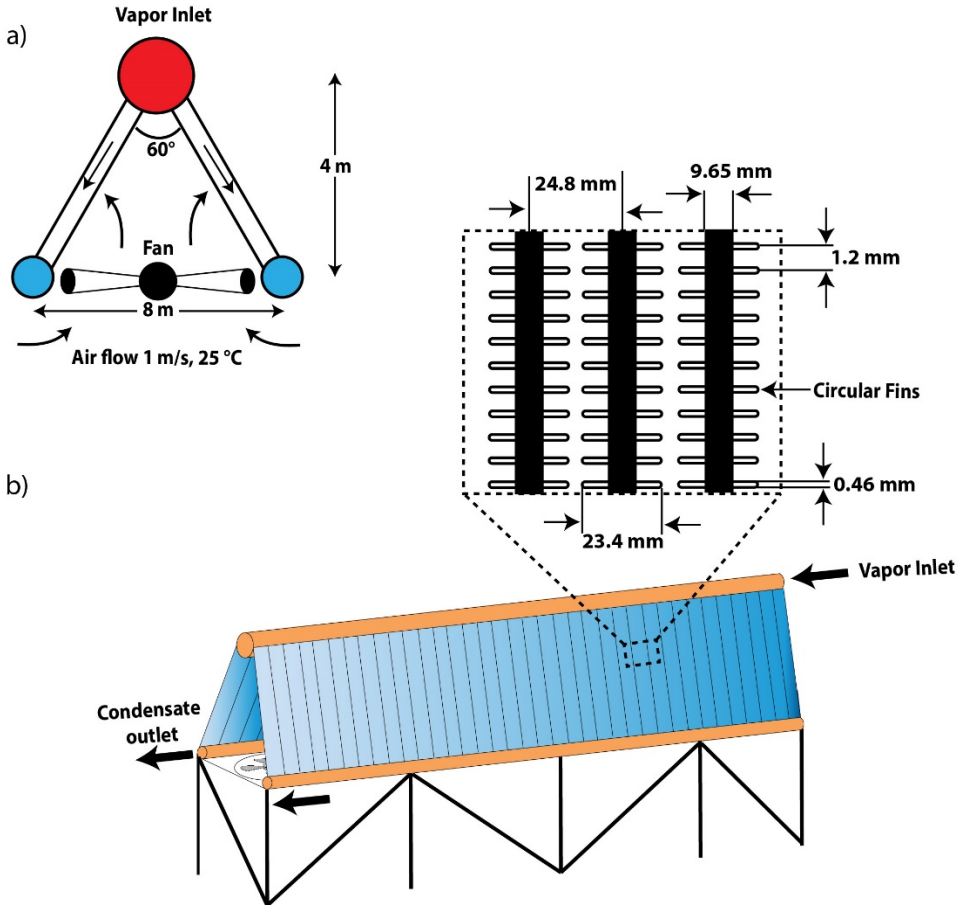

Figure 7 Schematic of the a) flow configuration in an A-frame ACC b) ACC system with tube geometries

The required flow rates for each refrigerant were evaluated by dividing the required cooling load (1055 kW) by the latent heat of vaporization at the evaporator temperature (0 °C). Since the

latent heat of vaporization of R454C is higher than that of R404A (Table 1), the resulting flow rate of R404A is 14% higher than that of R454C.

For the tubes in the ACC, the heat transfer was further modeled by dividing the tubes further into 25 segments. Thermal resistance networks were set up for each segment:

$$R_{tot} = R_{air} + R_{conduction} + R_{refrigerant}$$
$$R_{tot} = \frac{1}{h_{air} A_{so} \eta_{overall}} + \frac{\ln\left(\frac{d_o}{d_i}\right)}{2\pi l_{segment} k_{tube}} + \frac{1}{h_{ref} A_{si}} \quad (15)$$

where R_{air}, $R_{conduction}$ and $R_{refrigerant}$ are the thermal resistances due to air-side convection across the finned surface, conduction through the tube and refrigerant side convection, respectively. The number of tubes, and consequently the refrigerant flowrate in each tube, was varied such that the refrigerant enters the condenser with a 10 °C superheat and leaves the condenser with 5 °C subcooling. For both the refrigerants, two different approaches were tested: 1) the traditional approach which neglects the latent effects in the superheated and subcooled region, and 2) the non-equilibrium approach which predicts the heat transfer in the superheated and saturated regions using the Kondou & Hrnjak (2012) model, with the Gnielinski (1976) correlation for predictions in the subcooled region. For both the approaches, the mixture degradation was accounted for using the SBG correction. The total refrigerant-side heat transfer area was then evaluated for each refrigerant and each approach. The results are shown in the Figure 8. The application of non-equilibrium model reduced the heat exchanger area by 4.8% and 9.1% for R454C and R404A, respectively. This further highlights the advantage of the non-equilibrium approach. For water-cooled condensers, this decrease in area could be even more significant, as the condensation resistance becomes increasingly significant percentage of the overall heat transfer resistance.

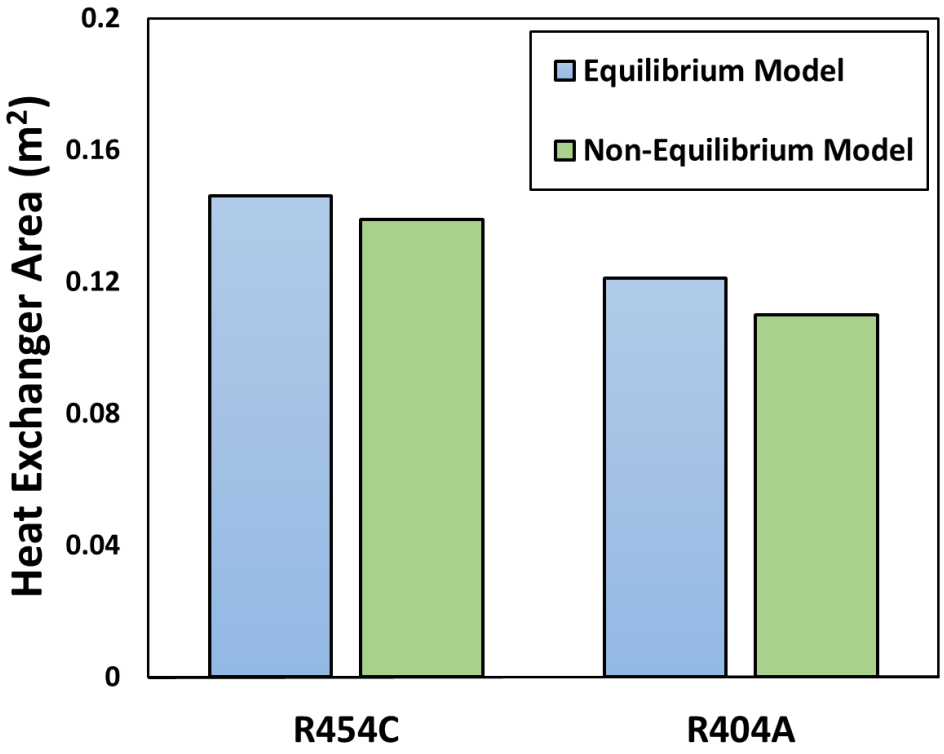

Figure 8 Refrigerant side heat exchanger area for R454C and R404A using the equilibrium and non-equilibrium models for constant cooling capacity (1055 kW).

Furthermore, the heat exchanger areas for R404A are 17% and 21% are lower than that of R454C for equilibrium and non-equilibrium approaches, respectively. There are two main reasons for the differences in the performance of these two refrigerants. Firstly, R404A operates at a higher mass flux, since it has a 14% lower latent heat of vaporization. Consequently, the heat transfer coefficients of R404A are higher. Secondly, as discussed earlier, R454C is a zeotropic mixture with a 6.8 °C temperature glide. As it undergoes condensation, the liquid/vapor interface temperature decreases and subsequently, the driving temperature difference to the process decreases, degrading heat transfer. Thus, while R454C has a higher the latent heat capacity and a higher liquid thermal conductivity, the degradation due to heat zeotropic condensation is significant and must be considered during design of newer systems. Furthermore, the Kondou & Hrnjak (2012) model was used to predict the non-equilibrium condensation because it agreed with

the data the best. However, this model assumes that the quality in the superheated region is equal to a constant value of 0.9999, which is not realistic. Thus, there is a further need for further research and new improved non-equilibrium models, which are based on realistic physical parameters that describe the process more accurately.

CONCLUSION

We investigated the non-equilibrium condensation of zeotropic refrigerant mixture R454C. R454C is a zeotropic refrigerant mixture (ΔT_{glide} = 6.5 °C) proposed to replace R404A in commercial refrigeration applications. Heat transfer coefficients were measured in the traditionally defined saturated region, as well in the upstream (superheated condensation) and downstream (subcooled condensation) regions in a 4.7 mm horizontal tube. Experiments were carried out at mass fluxes ranging from 100 – 500 kg m^{-2} s^{-1} at three different saturation conditions (40, 50 and 50 °C). Past researchers have developed non-equilibrium heat transfer models for pure fluids which consider the latent effects in the superheated and subcooled condensation regions, in addition to the saturated condensation regions. However, their applicability to zeotropic refrigerant mixtures is not clear. There is an additional mass transfer resistance associated with zeotropic condensation which is not captured by two-phase models developed for pure fluids. Based on the analysis conducted in this study, the following conclusions can be made:

- The Kondou & Hrnjak (2012) (superheated and saturated) model with the Gnielinski (1976) (subcooled) correlation exhibits the best agreement (MAPE = 9%) with the R454C data for complete condensation.
- In contrast, the conventional approach is also compared with the non-equilibrium models. The agreement of the measured data with traditional approach is poor (MAPE = 55%) in the superheated region but is satisfactory for complete condensation (MAPE = 15%).

- R454C heat transfer coefficients are similar to the R404A heat transfer coefficients at equal mass fluxes and same operating conditions.
- An air-cooled condenser is designed for a refrigeration system with a cooling capacity equal to 1055 kW using both the equilibrium and non-equilibrium approaches. For 454C, the heat exchanger area is 4.8% lower for the non-equilibrium model.
- Since R454C is a zeotropic mixture, its adoption requires addressing additional design challenges due to mixture degradation. The heat exchanger size for R454C is 17-21% greater than R404A for the same operating conditions.

NOMENCLATURE

Symbols

A	Area	(m^2)	α	Heat transfer coefficient	(kW m^{-2} K^{-1})
c_p	Specific heat	(kJ kg^{-1} K^{-1})	D	diameter	(m)
h	Enthalpy	(kJ kg^{-1})	$\dot{m}$	Mass flow rate	(kg s^{-1})
P	Pressure	(kPa)	P_r	Reduced Pressure	(-)
q''	Heat flux	(kW m^{-2})	$\dot{Q}$	Heat duty	(kW)
Re	Reynold's number	(-)	T	Temperature	(°C)
x	Thermodynamic quality	(-)	y	Bulk concentration	(-)

Subscripts

b	bulk	l	liquid
r	refrigerant	v	vapor
w	water	s	sensible
Sup	superficial	TP	Two-phase

DISCLOSURE

The authors declare that there is no conflict of interest regarding the publication of this article.

REFERENCES

Agarwal, R., & Hrnjak, P. (2014). Effect of sensible heat, condensation in superheated and subcooled region incorporated in unified model for heat rejection in condensers in horizontal round smooth tubes. *Applied Thermal Engineering*, *71*(1), 378–388. https://doi.org/10.1016/j.applthermaleng.2014.05.071

Arpagaus, C., Bless, F., Uhlmann, M., Schiffmann, J., & Bertsch, S. S. (2018). High temperature heat pumps: Market overview, state of the art, research status, refrigerants, and application potentials. *Energy*, *152*, 985–1010. https://doi.org/10.1016/j.energy.2018.03.166

ASHRAE. (2017). 2017 ASHRAE handbook: Fundamentals. In *2017 ASHRAE handbook : fundamentals*. American Society of Heating, Refrigeration and Air-Conditioning Engineers.

Azzolin, M., Berto, A., Bortolin, S., Moro, L., & Del Col, D. (2019). Condensation of ternary low GWP zeotropic mixtures inside channels. *International Journal of Refrigeration*, *103*, 77–90. https://doi.org/10.1016/j.ijrefrig.2019.03.021

Bell, K., & Ghaly, M. (1973). An approximate generalized design method for multicomponent/partial condenser. *American Institute of Chemical Engineers Symposium Series*, *69*, 72–79.

Cavallini, A., Censi, G., Del Col, D., Doretti, L., Longo, G. A., & Rossetto, L. (2002). Condensation of halogenated refrigerants inside smooth tubes. *HVAC and R Research*, *8*(4), 429–451. https://doi.org/10.1080/10789669.2002.10391299

Cavallini, A., Del Col, D., Doretti, L., Matkovic, M., Rossetto, L., Zilio, C., & Censi, G. (2006). Condensation in horizontal smooth tubes: A new heat transfer model for heat exchanger design. *Heat Transfer Engineering*, *27*(8), 31–38. https://doi.org/10.1080/01457630600793970

Del Col, D., Cavallini, A., & Thome, J. R. (2005). Condensation of Zeotropic Mixtures in Horizontal Tubes: New Simplified Heat Transfer Model Based on Flow Regimes. *Journal of Heat Transfer*, *127*(3), 221. https://doi.org/10.1115/1.1857951

Del Col, Davide, Azzolin, M., Bortolin, S., & Zilio, C. (2015). Two-phase pressure drop and condensation heat transfer of R32/R1234ze(E) non-azeotropic mixtures inside a single microchannel. *Science and Technology for the Built Environment*, *21*(5), 595–606. https://doi.org/10.1080/23744731.2015.1047718

Dittus, F. W., & Boelter, L. M. K. (1930). Heat transfer in automobile radiators of the tubular type. *University of California Pub. Eng.*, *2*, 443–461. https://doi.org/10.1097/AJP.0000000000000354

Dobson, M. K., & Chato, J. C. (1998). Condensation in Smooth Horizontal Tubes. *Journal of Heat Transfer*, *120*(1), 193. https://doi.org/10.1115/1.2830043

El Hajal, J., Thome, J. R., & Cavallini, A. (2003). Condensation in horizontal tubes, part 1: Two-phase flow pattern map. *International Journal of Heat and Mass Transfer*, *46*(18), 3349–3363. https://doi.org/10.1016/S0017-9310(03)00139-X

Fronk, B. M., & Garimella, S. (2013). In-tube condensation of zeotropic fluid mixtures: A review. *International Journal of Refrigeration*, *36*(2), 534–561. https://doi.org/10.1016/j.ijrefrig.2012.11.030

Fronk, B. M., & Garimella, S. (2016). Condensation of ammonia and high-temperature-glide zeotropic ammonia/water mixtures in minichannels – Part II: Heat transfer models. *International Journal of Heat and Mass Transfer*, *101*, 1357–1373. https://doi.org/10.1016/j.ijheatmasstransfer.2016.05.048

Garimella, S., Andresen, U. C., Mitra, B., Jiang, Y., & Fronk, B. M. (2016). Heat Transfer During Near-Critical-Pressure Condensation of Refrigerant Blends. *Journal of Heat Transfer*, *138*(5). https://doi.org/10.1115/1.4032294

Gnielinski, V. (1976). New Equations for Heat and Mass Transfer in Turbulent Pipe and Channel Flow. *International Chemical Engineering*.

Jacob, T. A., & Fronk, B. M. (2020a). *In-tube condensation data of R454C in a horizontal 4.7 mm ID tube*. Figshare. https://doi.org/doi.org/10.6084/m9.figshare.12235454.v1

Jacob, T. A., & Fronk, B. M. (2020b). Superheated Condensation of Refrigerant Mixtures R448A and R452A. *ASHRAE Annual Conference*, (Accepted).

Jacob, T. A., Matty, E. P., & Fronk, B. M. (2019). Experimental investigation of in-tube condensation of low GWP refrigerant R450A using a fiber optic distributed temperature sensor. *International Journal of Refrigeration*, *103*, 274–286. https://doi.org/10.1016/j.ijrefrig.2019.04.021

Jacob, T. A., Matty, E. P., & Fronk, B. M. (2020). Comparison of R404A condensation heat transfer and pressure drop with low global warming potential replacement candidates R448A and R452A. *International Journal of Refrigeration*, *116*, 9–22. https://doi.org/10.1016/j.ijrefrig.2020.03.014

Kays, W. M., & London, A. L. (1984). *Compact Heat Exchangers* (3rd ed.). McGraw Hill.

Kline, S., & McClintock, F. (1953). Describing uncertainties in single-sample experiments. *Mechanical Engineering*, *75*, 3–8.

Kondou, C., & Hrnjak, P. (2012). Condensation from superheated vapor flow of R744 and R410A at subcritical pressures in a horizontal smooth tube. *International Journal of Heat and Mass Transfer*,

55(11–12), 2779–2791. https://doi.org/10.1016/j.ijheatmasstransfer.2012.01.030

Kondou, C., Mishima, F., & Koyama, S. (2015). Condensation and evaporation of R32/R1234ze(E) and R744/R32/R1234ze(E) flow in horizontal microfin tubes. *Science and Technology for the Built Environment*, *21*(5), 564–577. https://doi.org/10.1080/23744731.2015.1023163

Lemmon, E. W., Bell, I. H., Huber, M. L., & Mclinden, M. O. (2018). *NIST Standard Reference Database 23: Reference Fluid Thermodynamic and Transport Properties-REFPROP, Version 10* (No. 10). National Institute of Standards and Technology.

Mota-Babiloni, A., Haro-Ortuño, J., Navarro-Esbrí, J., & Barragán-Cervera, Á. (2018). Experimental drop-in replacement of R404A for warm countries using the low GWP mixtures R454C and R455A. *International Journal of Refrigeration*. https://doi.org/10.1016/j.ijrefrig.2018.05.018

Shah, M. M. (1979). A general correlation for heat transfer during film condensation inside pipes. *International Journal of Heat and Mass Transfer*, *22*(4), 547–556. https://doi.org/10.1016/0017-9310(79)90058-9

Shah, M. M. (2016). Comprehensive correlations for heat transfer during condensation in conventional and mini/micro channels in all orientations. *International Journal of Refrigeration*, *67*, 22–41. https://doi.org/10.1016/j.ijrefrig.2016.03.014

Silver, L. (1947). Gas cooling with aqueous condensation. *Transactions of the Institution of Chemical Engineers*, *25*, 30–42.

Thome, J. R., El Hajal, J., & Cavallini, A. (2003). Condensation in horizontal tubes, part 2: New heat transfer model based on flow regimes. *International Journal of Heat and Mass Transfer*, *46*(18), 3365–3387. https://doi.org/10.1016/S0017-9310(03)00140-6

Webb, R. L. (1998). Convective condensation of superheated vapor. *Journal of Heat Transfer*, *120*(2), 418–421. https://doi.org/10.1115/1.2824266

Wu, X., Dang, C., Xu, S., & Hihara, E. (2019). State of the art on the flammability of hydrofluoroolefin (HFO) refrigerants. In *International Journal of Refrigeration* (Vol. 108, pp. 209–223). Elsevier Ltd. https://doi.org/10.1016/j.ijrefrig.2019.08.025

Xiao, J. (2019). *Non-equilibrium effects on in-tube condensation from superheated vapor*. University of Illinois at Urbana.

Xiao, J., & Hrnjak, P. (2017). A heat transfer model for condensation accounting for non-equilibrium effects. *International Journal of Heat and Mass Transfer*, *111*, 201–210. https://doi.org/10.1016/j.ijheatmasstransfer.2017.03.019

Xiao, J., & Hrnjak, P. (2019). Flow regimes during condensation from superheated vapor. *International Journal of Heat and Mass Transfer*, *132*, 301–308. https://doi.org/10.1016/j.ijheatmasstransfer.2018.12.016

Zhang, S., Wang, H., & Guo, T. (2010). Experimental investigation of moderately high temperature water source heat pump with non-azeotropic refrigerant mixtures. *Applied Energy*. https://doi.org/10.1016/j.apenergy.2009.11.001